

Micellization-Induced Conformational Change of a Chiral Proline Surfactant

Manli Deng,[†] Xu Huang,[†] Rongliang Wu,[‡] and Yilin Wang^{*,†}

Beijing National Laboratory for Molecular Sciences, Key Laboratory of Colloid and Interface Science, and State Key Laboratory of Polymer Physics and Chemistry, Institute of Chemistry, Chinese Academy of Sciences, Beijing 100190, People's Republic of China

Received: April 2, 2008; Revised Manuscript Received: May 12, 2008

A proline surfactant including two chiral carbons, sodium *N*-dodecanoyl-(4*R*)-hydroxy-*L*-prolinate (SDHP), has been synthesized, and its micellization behavior in aqueous solution has been investigated by ¹H NMR spectroscopy. Two conformational isomers of SDHP, namely, *Z* and *E*, are discriminated in the NMR time scale, and critical micelle concentration is derived for each isomer separately. The transformation from *E* to *Z* is observed upon micellization, and the amount of *Z* isomer is approximately three times that of *E* isomer in the equilibrated system. Moreover, the variation in chemical shifts with the surfactant concentration reveals the shielding effect of the carboxyl group on the syn-side protons of the pyrrolidine ring, which implies that the pyrrolidine rings arrange in a side-to-side manner and lie parallel to the plane of the carboxyl bonds in the neighboring molecules. The difference in the directions of the carbonyl group between *Z* and *E* isomers essentially determines their different micellization abilities and molecular arrangements in the micellization process.

Introduction

Amino acids, plentiful in nature and important actors in numerous life processes, have over the past decades found their way into the molecular structure of various surfactants. Most of these surfactants have *N*-acrylamino acid structures, with fatty acid residues as hydrophobic moieties connected to the amino groups of the amino acids. Due to the hindered rotation of the amide bond, the amino acid surfactant may have two conformational isomers, commonly named *Z* and *E*.^{1–3} Aggregation-induced *Z/E* isomerism of a surfactant has become an intriguing subject for the past decade.^{4,5} The conformationally mixed aggregates have been employed as enantioselector and chiral synthesis medium.^{6–8}

Mancini's group³ reported that an amino acid surfactant, sodium *N*-dodecanoyl-*L*-prolinate (SDP), could organize into a micelle with two separate domains on the basis of the *Z/E* stereochemical code. Moreover, they observed an enhanced proportion of *Z* isomer in aggregating conditions with respect to nonaggregating conditions. However, due to signal overcrowding, the variation of the molar ratio [*Z*]/[*E*] can not be traced with varying surfactant concentration. In the present work, we synthesized the amino acid surfactant sodium *N*-dodecanoyl-(4*R*)-hydroxy-*L*-prolinate (SDHP) and studied its micellization in aqueous solution by ¹H NMR spectroscopy. By introducing a hydroxyl group at the γ position of the pyrrolidine ring, new characteristics of ¹H NMR signals and more information about the micellization process have been obtained. The α -H signals for both isomers are clearly resolved and independent of other signals in the studied concentration range, from which the molar ratio [*Z*]/[*E*] can be followed as the concentration increases. Moreover, signals of the four δ protons in the two isomers of SDHP are resolved, making it possible to determine the critical micelle concentration (CMC) for each isomer. The changes in the observed chemical shifts of the SDHP protons shed some

light on the intermolecular interactions and conformational changes in the micelles. A model for the possible molecular arrangement in the micelle is proposed.

Experimental Section

Materials. (4*R*)-hydroxy-*L*-proline was purchased from GL Biochem (Shanghai) Ltd., and the purity was above 99%. All of the organic solvents and inorganic reagents were purchased from Beijing Chemical Co. and were of analytical grade. Deuterium oxide (99.9%) was purchased from CIL Cambridge Isotope Laboratories.

Synthesis. SDHP was synthesized according to literature procedures.^{9,10} Dodecanoyl chloride was added dropwise to an ice-bathed solution containing 1 M aqueous sodium hydroxide and 10% excess (4*R*)-hydroxy-*L*-proline. The reaction mixture was stirred at room temperature for 5 h. Concentrated hydrochloric acid was added to the mixture to bring the pH to 1. Floccular precipitate was extracted by ethyl ether, and the extract was washed with 5% hydrochloric acid and water and then dried. The TLC-pure product of *N*-dodecanoyl-(4*R*)-hydroxy-*L*-proline was obtained as a wax-like solid after solvent evaporation in vacuum and was neutralized with an equivalent of sodium hydroxide to give SDHP. Crystallization from ethyl acetate gave pure SDHP as white solid in 82% yield. ¹H NMR (600 MHz, D₂O): δ = 0.877 (t, 3H, 12-CH₃), 1.293 (m, 16H, 4~11CH₂), 1.599 (m, 2H, 3-CH₂), 2.058–2.446 (m, 4H, 2-CH₂ and β -CH₂), 3.568–3.809 (m, 2H, δ -CH₂), 4.332 and 4.452 (t, 1H, α -H), 4.514 and 4.552 (br, 1H, γ -H). MS-ESI (*m/z*): calcd, 335.2; found, 312.2 (M-23). Anal. Calcd for C₁₇H₃₀NNaO₄·H₂O: C, 57.77; H, 9.13; N, 3.96. Found: C, 57.15; H, 9.28; N, 3.99.

NMR. NMR spectra were recorded at 25.0 \pm 0.5 °C on Bruker AV 400 and Bruker AV 600 FT-NMR spectrometers operating at 400.1 and 600.1 MHz, respectively. The peaks were referenced with respect to the residual proton signal of D₂O (δ = 4.79 ppm). In all NMR experiments, the numbers of scans were adjusted to achieve good signal-to-noise ratios depending on surfactant concentration. In the studied concentration range of the SDHP aqueous solutions, the pH varies from 7.13 to 8.33,

* To whom the correspondence should be addressed. E-mail: yilinwang@iccas.ac.cn.

[†] Key Laboratory of Colloid and Interface Science.

[‡] State Key Laboratory of Polymer Physics and Chemistry.

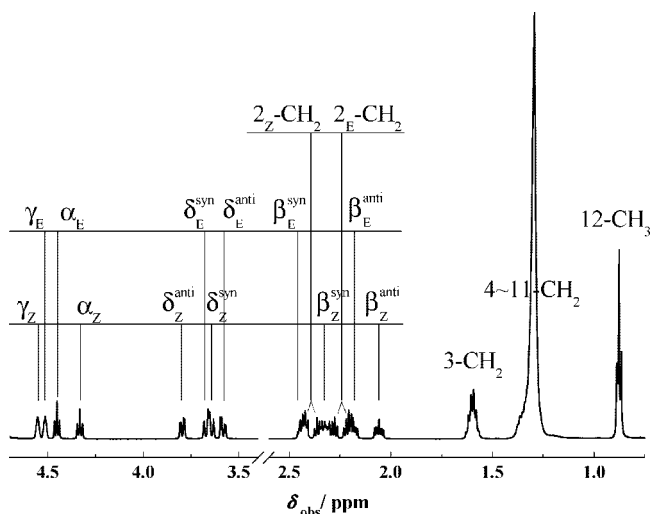


Figure 1. ^1H NMR spectrum of 10 mM SDHP in D_2O and the assignments for all of the signals.

which do not affect the ionization degree of SDHP obviously since the pK_a value of SDHP is 4.9 determined by pH titration.

Isothermal Titration Microcalorimetry (ITC). The calorimetric measurements were performed in a TAM 2277–201 microcalorimetric system (Thermometric AB, Järfälla, Sweden) with a 1 mL stainless steel sample cell at 25.00 ± 0.01 °C. The detailed procedure was described previously.^{11,12} The observed enthalpies (ΔH_{obs}) were obtained by integrating the areas of the peaks in the plot of thermal power against time.

Steady-State Fluorescence Measurement. Pyrene (1 μM) was used as probe to determine the CMC from measurement of the pyrene polarity index I_1/I_3 , which is the ratio of the intensities of the first and the third vibronic peaks in the fluorescence spectrum.¹³ Pyrene was excited at 335 nm and the emission spectra were scanned from 350 to 550 nm. The measurements were conducted with a Hitachi F-4500 spectrofluorometer at 25.0 ± 0.5 °C.

Results and Discussion

The ^1H NMR spectrum of 10.0 mM SDHP in D_2O is presented in Figure 1. It is easy to ascribe the three resonance lines at upper field to the protons in the alkyl chain of SDHP, whereas the assignments of other signals are rather complicated. Because the pyrrolidine ring has two chiral carbon atoms, each proton in the ring generates a different signal. Besides, each signal splits into two groups due to the presence of the amide bond next to the ring. These two-group peaks correspond to two conformational isomers, that is, *Z* and *E* as illustrated in Figure 2. The definitions of the protons are referred to the position of α -H in the pyrrolidine ring.

With the aid of ^1H – ^1H COSY and NOESY experiments performed on 10.0 mM SDHP in D_2O , all of the ^1H NMR signals can be assigned. From the ^1H – ^1H COSY spectrum (Figure 3a), the signals can be divided into two set of peaks, and the related signals can be ascribed to certain protons in SDHP molecule. Moreover, from the signals marked with red circles in NOESY spectrum (Figure 3b), these two set of peaks can be assigned to the corresponding conformations, respectively. The overall assignments are marked above the signals of the ^1H NMR spectrum in Figure 1, and the calculated coupling constants (J) are listed in Table 1. The α -H signals show a clear triplet for each isomer, indicating the two magnetically nonequivalent β protons have the same coupling

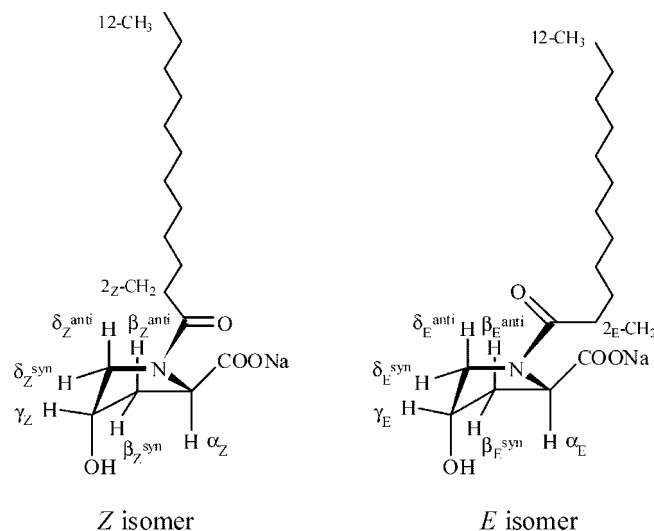


Figure 2. *Z* and *E* isomers of SDHP and the definitions of the protons.

constant $J_{\alpha-\beta}$. Contrarily, the β -CH₂ signals include four groups of multiple peaks and overlap with the 2-CH₂ signals next to the amide group in the alkyl chain. Hereafter, β -CH₂ and 2-CH₂ signals are not discussed in the following text due to their overlapping. The δ protons resonate as four signals, two for each isomer. The signals of δ_Z^{anti} and δ_E^{anti} are a well-resolved doublet of doublets, from which the coupling constants $J_{\delta-\delta}$ and $J_{\delta-\gamma}$ could be obtained. Notably, the coupling constants for *Z* isomer have the same values as those for *E* isomer except $J_{\delta-\delta}$, which is larger than the latter. This suggests that the interaction between the two δ protons in *E* isomer is a little stronger than that in *Z* isomer, probably due to the influence of intramolecular carbonyl group. In addition, the signals of δ_Z^{syn} and δ_E^{syn} are partially overlapped and not as well-resolved as those of δ_Z^{anti} and δ_E^{anti} . Although the W-like long-range couplings of δ_E^{syn} – β_E^{syn} and δ_Z^{syn} – β_Z^{syn} are evidenced by the ^1H – ^1H COSY spectrum as marked in Figure 3a, the coupling constants between them is too small to be determined.

The ^1H NMR spectra as a function of SDHP concentration are presented in Figure 4, providing fruitful information on the micellization process of SDHP. The ^1H NMR chemical shift can be used to determine the CMC of the surfactant.^{14–16} Under fast exchange in the NMR time scale, the observed chemical shift for the corresponding proton (δ_{obs}) can be expressed as the weighted average of the chemical shifts of the monomer (δ_{mon}) and the aggregated form (δ_{mic}),

$$\delta_{\text{obs}} = \delta_{\text{mon}} \left(\frac{C_{\text{mon}}}{C} \right) + \delta_{\text{mic}} \left(\frac{C_{\text{mic}}}{C} \right) \quad (1)$$

where C_{mon} , C_{mic} , and C are the concentrations of the surfactant molecules existing as monomers, micelles, and in total in solution. If the monomer concentration is assumed to be constant above CMC, then

$$\delta_{\text{obs}} = \delta_{\text{mic}} - \left(\frac{\text{CMC}}{C} \right) (\delta_{\text{mic}} - \delta_{\text{mon}}) \quad (2)$$

Therefore, a plot of δ_{obs} versus $1/C$ should yield two straight lines below and above the CMC, and the intersection of these lines corresponds to the CMC. Figure 5 shows such plots for the protons of 12-CH₃, δ_Z^{anti} , and δ_E^{anti} . The signal of 12-CH₃ is shared by *Z* and *E* isomers, thus the CMC derived from this signal should be regarded as the apparent CMC for the conformationally mixed system. The value of 18.5 mM is in

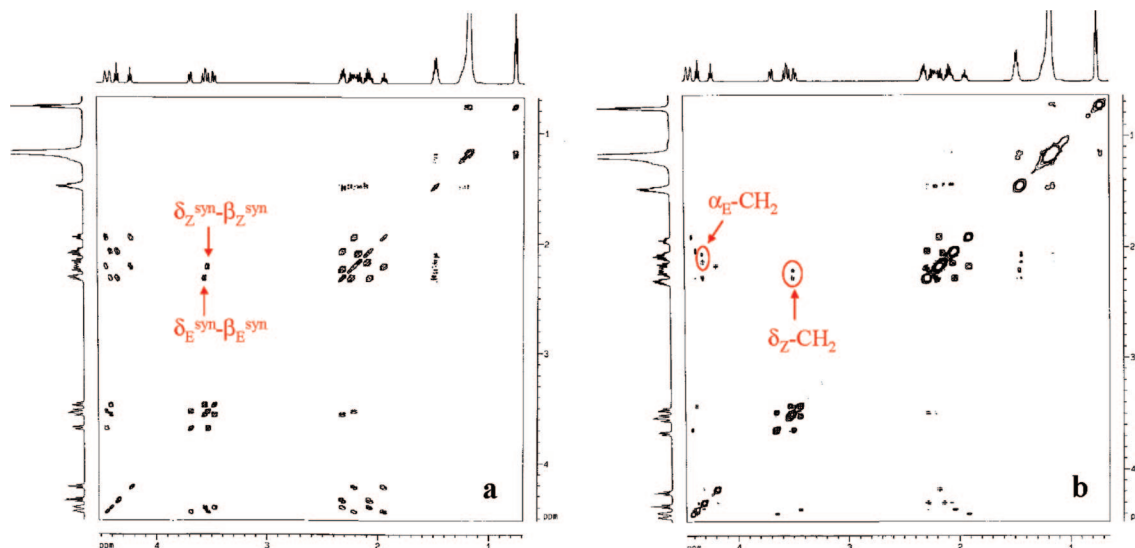


Figure 3. 2D NMR spectra of 10 mM SDHP in D₂O. (a) ¹H–¹H COSY spectrum and (b) NOESY spectrum.

TABLE 1: Coupling Constants Derived from ¹H NMR Signals

<i>J</i> (Hz)	<i>J</i> _{α-β}	<i>J</i> _{β-β}	<i>J</i> _{β-δ}	<i>J</i> _{δ-δ}	<i>J</i> _{δ-γ}
<i>Z</i>	8.4	13.2	4.8	11.4	4.2
<i>E</i>	8.4	13.2	4.8	12.6	4.2

good agreement with the results of ITC and fluorescence spectroscopy (Figure S1). As to the δ protons, *Z* and *E* isomers exhibit distinctive signals. Supposing there was only one isomer in the system, the CMC of *Z* or *E* isomer could be independently derived from the δ_Z or δ_E signals of the corresponding isomer. The CMC values of *Z* isomer and *E* isomer under such supposition are obtained as 17.7 mM and 20.8 mM, respectively. In fact, the two isomers exist simultaneously in the system. Therefore, the apparent CMC of the system should be the weighted contributions from both of the isomers,

$$CMC = CMC_Z f_Z + CMC_E f_E \quad (3)$$

where f_Z and f_E are the mole fractions of *Z* and *E* isomers in the solution and are obtained by integration of the signals of *Z* and

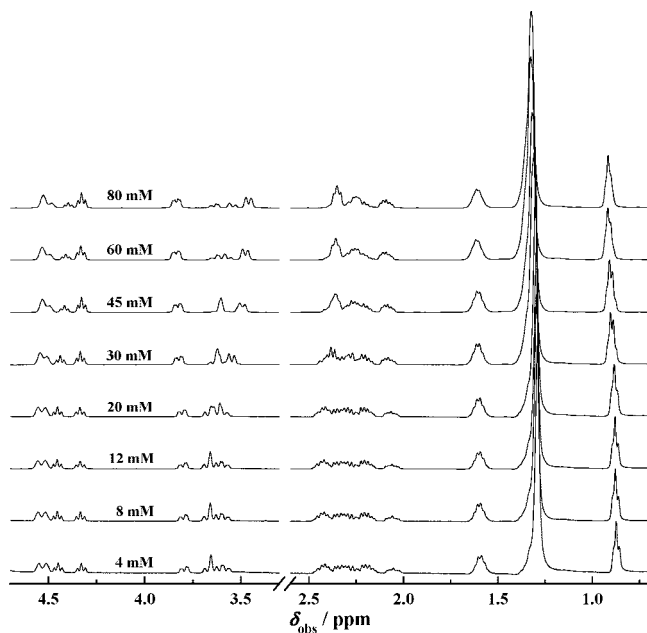


Figure 4. ¹H NMR spectra of SDHP with variation of concentration (indicated above the curves).

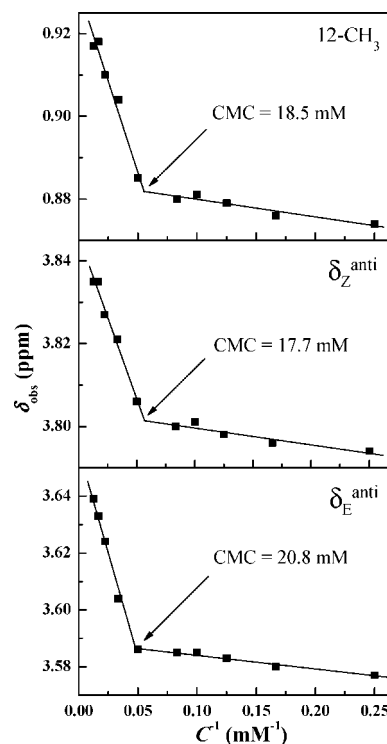


Figure 5. Variation of the observed chemical shifts of 12-CH₃, δ_Z^{anti} , and δ_E^{anti} with the reciprocal concentration of SDHP.

E isomers (discussed below). The apparent CMC calculated accordingly is also 18.5 mM, which is amazingly consistent with the apparent CMC obtained from 12-CH₃ signal. In addition, the CMC for each isomer and the calculated apparent CMC are determined in the same way from the signals of γ -H for comparison, and the values are listed in Table S2 in Supporting Information. It is noted that the difference between the CMC values of *Z* and *E* isomers is beyond experimental error, and this demonstrates that the micellization ability of *Z* isomer is stronger than that of *E* isomer.

Additionally, the integral areas of the ¹H NMR signals of *Z* and *E* isomers can be used to calculate the isomer composition in the solution.^{2–4} Since the signals of α -H are well-resolved and independent of any other signals for both isomers, the contents of *Z* and *E* isomers can be followed in the whole

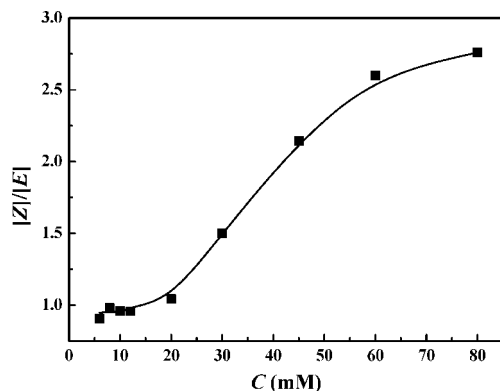


Figure 6. Variation of the mole concentration ratio of Z isomer to E isomer ($[Z]/[E]$) with the SDHP concentration.

concentration range investigated. The calculated mole concentration ratio $[Z]/[E]$ is plotted against the surfactant concentration in Figure 6, and the solid line is a sigmoidal fit to the data. At low concentrations below CMC, the ratio remains a nearly constant value close to 1, indicating that *E* isomer and *Z* isomer exist equally in the monomer solution. As the concentration increases to the apparent CMC value, the ratio rises steeply. Finally, the molar fraction of *Z* approaches almost three times that of *E* at much higher surfactant concentrations, where the $[Z]/[E]$ plot levels off and the transformation completes. Hence, it can be concluded that *E* isomer is unfavorable in micelles and starts to transform into *Z* isomer as soon as the micellization takes place. The above phenomenon should originate from the difference in the directions of carbonyl groups within the two isomers. For *Z* isomer, both the carbonyl and the carboxyl groups in the rigid headgroup can be exposed to water simultaneously, and thus, *Z* can adopt a structured and tight organization upon micellization. Therefore, the *Z* isomer is preferred in the micellar solution. While for *E* isomer, the carbonyl and carboxyl groups point to opposite directions. One of these hydrophilic groups is favorably exposed to bulk water at the micelle surface, and the other has to be buried under the surface. Such an arrangement may result in deeper penetration of water molecules into the micelle and make it disordered. Besides, the larger hydrophilic area of the *E* isomer might make it favor the monomer state in the solution.

Furthermore, the variation of the chemical shifts with the surfactant concentration supply additional information on the intermolecular interactions in the micellization process.^{17–19} As shown in Figure 4, below CMC, the chemical shifts of all signals scarcely change with the surfactant concentration, whereas above CMC, nearly all of the resonances experience relatively large shifts. For the protons in the alkyl chain, the signals shift downfield as the surfactant concentration increases, while the situation for the protons in the pyrrolidine ring is more intricate. Generally, the signals of protons in the *Z* isomer change in the same trend as for their counterparts in the *E* isomer. The most significant changes in the chemical shifts beyond CMC are observed in the signals of δ protons. The decreasing sequence of the chemical shifts for the δ protons is $\delta_{Z}^{\text{anti}} > \delta_{E}^{\text{syn}} > \delta_{Z}^{\text{syn}} > \delta_{E}^{\text{anti}}$ below CMC, but it turns into $\delta_{Z}^{\text{anti}} > \delta_{E}^{\text{anti}} > \delta_{E}^{\text{syn}} > \delta_{Z}^{\text{syn}}$ above 3CMC. This signal crossing could be identified from the characteristic doublet of doublets of δ_{Z}^{anti} and δ_{E}^{anti} . Moreover, the changes in the chemical shifts of the δ protons are sterically dependent. The signals of the δ_{Z}^{syn} and δ_{E}^{syn} protons at the syn-side of α -H move upfield, while the signals of the δ_{Z}^{anti} and δ_{E}^{anti} protons at the anti-side of α -H move downfield. The shifting extents of the signals are shown in Figure 7. The upfield shift of γ -H and downfield shift of 12-CH₃

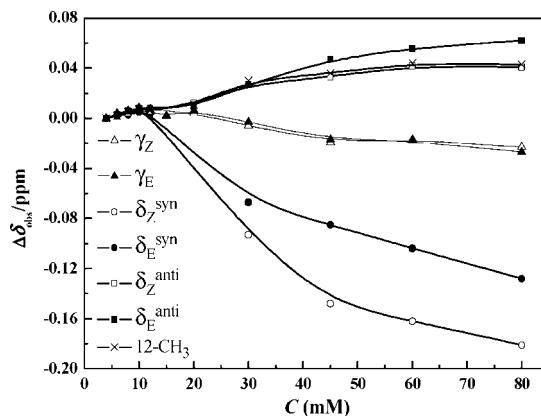


Figure 7. Changes in the observed chemical shifts of the protons in the pyrrolidine ring and 12-CH₃ in the alkyl chain with the SDHP concentration.

are also included for comparison. It is obvious that the extent of upfield shifts of the δ^{syn} signals is much larger than that of the downfield shifts of the δ^{anti} signals. Also, the difference in the magnitudes of the upfield shifts between the δ_Z^{syn} and the δ_E^{syn} signals is dramatically large compared with that between the γ_Z and the γ_E signals.

The magnitude and nature of these variations in the chemical shifts reflect the changes in the molecular conformation, the environment of the protons sensed, and their extent of evolution during micellization. Normally, changes in the chemical shifts with micellization are discussed in terms of medium effects and conformation effects.^{20–22} The former is caused by monomer transfer from water into micelle, where surfactant alkyl chains are immersed into a hydrophobic core, and the hydrophilic headgroups are solvated by interfacial water, whose polarity is similar to that of methanol and ethanol.^{23,24} The decrease of polarity upon solvation leads to a downfield shift. While the small upfield shifts of γ signals indicate an increase in the polarity of the microenvironment of the γ -H. It might be caused by the formation of hydrogen bond between the hydroxyl group and the carboxyl group of the adjacent molecules during the micellization process. The same change extents for the γ_Z and γ_E signals implies the hydroxyl group plays the same role in the *Z* and *E* isomers. Concerning the conformation effect, micellization is always accompanied by a gauche-to-trans conformational change of the alkyl chain. The increasing proportion of trans conformations also leads to a downfield shift, and the largest magnitude occurs for the protons in the middle of the alkyl chain.^{25,26} For SDHP, the above two effects account for the downfield shifts observed in the signals of all protons in the alkyl chain and δ^{anti} protons in the pyrrolidine ring. Yet the prominent upfield shifts of the δ^{syn} signals indicate a shielding effect, which may arise from the anisotropy of the carboxyl and/or the carbonyl in the neighboring SDHP molecules. The anisotropic effect has quite precise geometrical requirements. Only those protons situated in the shielding cone perpendicular to the π electron plane can be substantially shifted. The larger shifts of the δ_Z^{syn} signals than those of δ_E^{syn} imply a greater involvement of the δ_Z^{syn} proton in the shielding cone.

On the basis of the above characterization of the micellization of SDHP in aqueous solution, we tentatively propose a model for the possible molecular arrangement in SDHP micelles, as illustrated in Figure 8. (i) The alkyl chains of SDHP molecules aggregate into a hydrophobic core, leaving the pyrrolidine rings stack up within the solvated palisade. (ii) The negatively charged carboxyl groups are favorably exposed to bulk water, and stay apart from

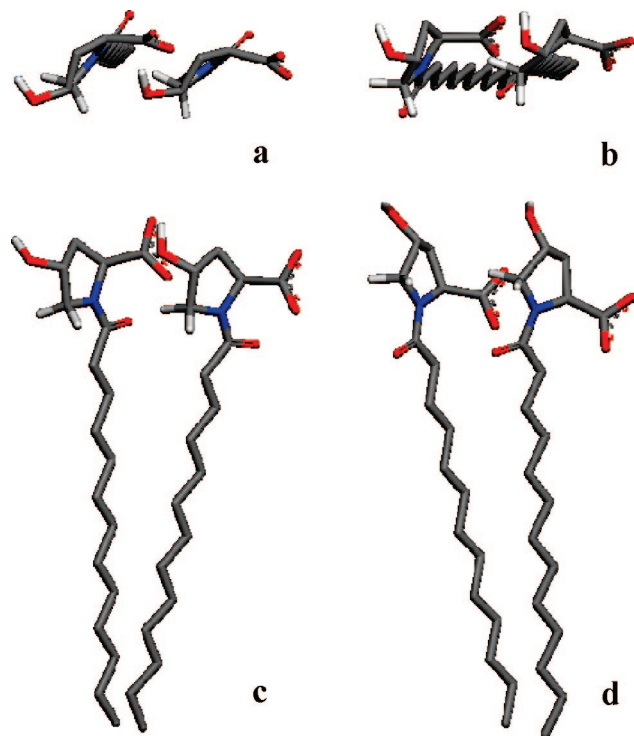


Figure 8. Stick representation of the proposed molecular arrangement in a SDHP micelle: (a,b), top view of *Z* and *E* isomers; (c,d), side view of *Z* and *E* isomers, respectively. Only δ protons are displayed.

each other due to electrostatic repulsion. And it is also possible to form an intermolecular hydrogen bond between the carboxyl group and the hydroxyl group. This hydrophilic preference, electrostatic repulsion, and intermolecular hydrogen bond might facilitate a “syn-side to anti-side” arrangement for the adjacent rings. (iii) The π electron cloud of the carboxyl group lies in parallel with the adjacent pyrrolidine ring, and the shielding cone could consequently cover the syn-side protons (β^{syn} and δ^{syn}) of the adjacent ring, leading to the upfield shift of these signals. (iv) The micelles may be organized into two separate domains of *Z* and *E* isomers, which has been suggested by Mancini and co-workers.^{3,5} In the domain of *E* isomer, the δ^{Esyn} protons are beyond the shielding regime of the carbonyl group and are only shielded by the carboxyl group. While in the domain of *Z* isomer, the δ^{Zsyn} protons are located in the shielding cone of the carboxyl groups and the carbonyl groups in the adjacent SDHP molecules. This accounts for the greater magnitude of the upfield shifts of the signals of δ^{Zsyn} with respect to those of δ^{Zsyn} . (v) The difference in the direction of the carbonyl group between *Z* and *E* isomers essentially determines their different micellization abilities. The opposite directions of the carbonyl group and the carboxyl group within *E* isomer enlarge the hydrophilic area of the amphiphile, which reduces the micellization ability of *E* isomer.

Conclusions

A chiral amino acid surfactant containing prolyl structure, SDHP, has been synthesized and characterized by complementary ^1H – ^1H COSY and NOESY spectroscopy. The micelle formation of SDHP has been studied by ^1H NMR, ITC, and fluorescence spectroscopy. The CMCs of the *Z* and *E* isomers of SDHP were determined to be 17.7 mM and 20.8 mM from the ^1H NMR signals of δ^{Zanti} and δ^{Eanti} , respectively. The apparent CMC calculated using the CMC values of the two isomers gives the same value as that experimentally derived

from the signals shared by the two isomers. The *Z* isomer is more populated in micelle than the *E* isomer. The transformation from *E* to *Z* conformation is observed upon micellization and reaches equilibrium well-above the CMC, where the molar fraction of *Z* isomer is about three times that of *E* isomer. Moreover, it can be inferred from the NMR data that the syn-side protons experience the π electron anisotropy of the carboxyl group, which implies that in the micelles the pyrrolidine rings arrange in a side-to-side manner and the carboxyl groups lie in parallel with the neighboring pyrrolidine rings. This work helps to understand the micellization-induced conformational transformations of chiral amino acid surfactants.

Acknowledgment. We are grateful for financial support from the National Natural Science Foundation of China and National Basic Research Program of China (Grants 20633010 and 2005cb221300).

Supporting Information Available: Figures of the results about the SDHP micellization in aqueous solution studied by ITC and fluorescence spectroscopy, table of the pH values at different SDHP concentrations, and table of the CMC values determined from different proton signals of NMR. This material is available free of charge via the Internet at <http://pubs.acs.org>.

References and Notes

- (1) Taylor, C. M.; Hardré, R.; Edwards, P. J. B. *J. Org. Chem.* **2005**, *70*, 1306–1315.
- (2) Andreotti, A. M. *Biochemistry* **2003**, *42*, 9515–9524.
- (3) Borocci, S.; Mancini, G.; Cerichelli, G.; Luchetti, L. *Langmuir* **1999**, *15*, 2627–2630.
- (4) Ambühl, M.; Bangerter, F.; Luisi, P. L.; Skrabal, P.; Watzke, H. J. *Langmuir* **1993**, *9*, 36–38.
- (5) Cerichelli, G.; Luchetti, L.; Mancini, G. *Langmuir* **1997**, *13*, 4767–4769.
- (6) Belogi, G.; Croce, M.; Mancini, G. *Langmuir* **1997**, *13*, 2903–2904.
- (7) Bombelli, C.; Borocci, S.; Lupi, F.; Mancini, G.; Mannina, L.; Segre, A. L.; Viel, S. *J. Am. Chem. Soc.* **2004**, *126*, 13354–13362.
- (8) Gübitz, G.; Schmid, M. G. *Electrophoresis* **2004**, *23*, 3981–3996.
- (9) Miyagishi, S.; Nishida, M. *J. Colloid Interface Sci.* **1978**, *65*, 380–386.
- (10) Jungermann, E.; Gerecht, J. F.; Krems, I. J. *J. Am. Chem. Soc.* **1956**, *78*, 172–174.
- (11) Li, Y.; Reeve, J.; Wang, Y.; Thomas, R. K.; Wang, J.; Yan, H. *J. Phys. Chem. B* **2005**, *109*, 16070–16074.
- (12) Li, Y.; Li, P.; Wang, J.; Wang, Y.; Yan, H.; Thomas, R. K. *Langmuir* **2005**, *21*, 6703–6706.
- (13) Zana, R. In *Surfactant Solutions: New Methods of Investigation*; Zana, R., Ed.; Marcel Dekker: New York, 1987; pp 241–294.
- (14) Faure, A.; Tistchenko, A. M.; Zemb, T.; Chachaty, C. *J. Phys. Chem.* **1985**, *89*, 3373–3378.
- (15) Zhao, J.; Fung, B. M. *Langmuir* **1993**, *9*, 1228–1231.
- (16) Davey, T. M.; Ducker, W. A.; Hayman, A. R. *Langmuir* **2000**, *16*, 2430–2435.
- (17) Das, S.; Bhirud, R. G.; Nayyar, N.; Narayan, K. S.; Kumar, V. V. *J. Phys. Chem.* **1992**, *96*, 7454–7457.
- (18) Goon, P.; Das, S.; Clemett, C. J.; Tiddy, G. J. T.; Kumar, V. V. *Langmuir* **1997**, *13*, 5577–5582.
- (19) Xing, H.; Lin, S.; Yan, P.; Xiao, J.; Chen, Y. *J. Phys. Chem. B* **2007**, *111*, 8089–8095.
- (20) Persson, B.-O.; Drakenberg, T.; Lindman, B. *J. Phys. Chem.* **1976**, *80*, 2124–2125.
- (21) Shimizu, S.; Pires, P. A. R.; El Seoud, O. A. *Langmuir* **2003**, *19*, 9645–9652.
- (22) Huang, X.; Han, Y.; Wang, Y.; Wang, Y. *J. Phys. Chem. B* **2007**, *111*, 12439–12446.
- (23) Tada, E. B.; Novaki, L. P.; El Seoud, O. A. *Langmuir* **2001**, *17*, 652–658.
- (24) Romsted, L. S. In *Surfactants in Solution*; Mittal, K. L., Lindman, B., Eds.; Plenum Press: New York, 1984; Vol. 2, pp 1015–1068.
- (25) Levy, G. C.; Komoroski, R. A.; Halstead, J. A. *J. Am. Chem. Soc.* **1974**, *96*, 5456–5461.
- (26) Persson, B.-O.; Drakenberg, T.; Lindman, B. *J. Phys. Chem.* **1979**, *83*, 3011–3015.